JOURNAL OF MAGNETIC RESONANCE **135,** 478–486 (1998)
ARTICLE NO. MN981588

# Pulsed-Field-Gradient Measurements of Time-Dependent Gas Diffusion

Ross W. Mair,* David G. Cory,† Sharon Peled,† Ching-Hua Tseng,*,‡ Samuel Patz,‡ and Ronald L. Walsworth*,[1]

*Harvard–Smithsonian Center for Astrophysics, Cambridge, Massachusetts 02138; †Department of Nuclear Engineering, Massachusetts Institute of Technology, Cambridge, Massachusetts 02139; and ‡Department of Radiology, Brigham and Women's Hospital and Harvard Medical School, Boston, Massachusetts 02115

Received March 6, 1998; revised August 11, 1998

**Pulsed-field-gradient NMR techniques are demonstrated for measurements of time-dependent gas diffusion. The standard PGSE technique and variants, applied to a free gas mixture of thermally polarized xenon and $O_2$, are found to provide a reproducible measure of the xenon diffusion coefficient ($5.71 \times 10^{-6}$ m$^2$ s$^{-1}$ for 1 atm of pure xenon), in excellent agreement with previous, non-NMR measurements. The utility of pulsed-field-gradient NMR techniques is demonstrated by the first measurement of time-dependent (i.e., restricted) gas diffusion inside a porous medium (a random pack of glass beads), with results that agree well with theory. Two modified NMR pulse sequences derived from the PGSE technique (named the Pulsed Gradient Echo, or PGE, and the Pulsed Gradient Multiple Spin Echo, or PGMSE) are also applied to measurements of time dependent diffusion of laser polarized xenon gas, with results in good agreement with previous measurements on thermally polarized gas. The PGMSE technique is found to be superior to the PGE method, and to standard PGSE techniques and variants, for efficiently measuring laser polarized noble gas diffusion over a wide range of diffusion times.** 

*Key Words:* **laser polarized noble gas; PGSE technique; gas diffusion; restricted diffusion; porous media.**

## INTRODUCTION

Measurements of time-dependent liquid diffusion using pulsed-field-gradient NMR techniques have many important applications, ranging from colloidal/emulsion characterization (*1, 2*), to probes of porous microstructure in systems such as bead packs or reservoir rocks saturated with water (*3, 4*). Until now, pulsed-field-gradient NMR techniques have not been used to measure time-dependent gas diffusion, perhaps because of the small NMR signals provided by thermally polarized gases. Indeed, until a few years ago, gas-phase NMR had been a very limited field of study. The most common applications had been the study of relaxation parameters throughout the phase diagram of fluorinated or noble gases (*5, 6*), and the use of fluorinated gases to image porous and biological samples (*7–9*). Recently, however, there has been a surge of interest in gas-phase NMR, following the application of optical pumping techniques using lasers to produce large nuclear spin polarizations ($\gtrsim$10%) in the spin $\frac{1}{2}$ noble gases ($^{129}$Xe and $^{3}$He) (*10*). To date, much of the interest in laser polarized noble gas NMR has focused on imaging, for example, imaging of the lung gas space in animals (*11*) and humans (*12*), as well as enhancement of signals in contact with the laser polarized gas via cross-polarization, either on surfaces or in the dissolved state (*13*).

We believe pulsed-field-gradient NMR measurements of time-dependent noble gas diffusion will also have wide utility in both biomedical and non-biomedical systems, for example, in determining the fluid permeability and surface area-to-volume ratio of porous and granular media (lung airways, reservoir rocks, sand piles, etc.). NMR studies of liquid-saturated porous and granular media provide important, but limited, information on sample microstructure for length scales below the resolution obtainable with direct MRI techniques (*4, 14*). In particular, pulsed-field-gradient NMR studies of water diffusion in porous reservoir rocks and packed bead systems have shown that water NMR signals decay due to surface relaxation faster than the time for water molecules to diffuse between pores (*15*). Thus imbibed-liquid NMR can accurately measure the porosity of such systems, but is generally poor at determining microstructural detail over multi-pore length scales ($>$100 $\mu$m in reservoir rocks) (*3, 15*), information that is crucial in determining important properties such as fluid permeability in porous media. However, pulsed-field-gradient NMR measurements of time dependent diffusion of imbibed noble gas should be a good probe of multi-pore length scales because of (i) rapid gas diffusion; and (ii) the weak interaction of noble gas atoms with surfaces (and the resultant low surface relaxation of noble gas spins).

With the advent of laser polarized noble gas NMR, several recent publications have addressed the measurement of noble gas spin-relaxation times and diffusion coefficients while accounting for the non-renewable spin-polarization provided by the laser polarization technique (*16–21*). However, in none of these publications have pulsed-field-gradient techniques been employed in a time dependent manner; hence work to date is applicable only to spatially homogeneous (i.e., free or unre-

[1] To whom correspondence should be addressed. Fax: (617) 496 7690, E-mail: rwalsworth@cfa.harvard.edu.



1090-7807/98 $25.00

stricted) diffusion. In several of these time-independent noble gas diffusion measurements, a simple one-dimensional imaging technique was used, bleaching a hole in the gas magnetization and watching the signal return over time (*16, 18, 21*). Most recently (*19–21*), a more sophisticated method has been employed, based on the original technique of Carr and Purcell (*22*) for measuring unrestricted diffusion in a constant magnetic field gradient using a spin-echo. In these recent experiments (*19–21*), the sign of the gradient was reversed midway through the measurement period and the resulting gradient echo refocused the spins in place of an RF pulse. Nevertheless, this modified Carr–Purcell method remains essentially a constant gradient technique, and thus does not allow the measurement of time-dependent gas diffusion, as do the pulsed-field-gradient techniques based on the method of Stejskal and Tanner (*23*). (Note that time-independent diffusion of thermally polarized gases has also been measured by NMR, sporadically, over the years (*24–27*); and in most cases (*25–27*) the method used was the Carr–Purcell constant gradient technique (*22*).)

In contrast, for liquids, techniques based on the method of Stejskal and Tanner (*23*) have displaced constant gradient techniques (e.g., Carr–Purcell) as the method of choice for accurate diffusion measurement by NMR. In particular, the Pulsed Gradient Spin Echo (PGSE) technique (*23*) and its variants (*28*) are now widely used for time dependent diffusion measurements in liquids and related systems (*2, 29, 30*). For example, "diffraction-like" effects observed in PGSE measurements of restricted liquid diffusion yield accurate determinations of pore sizes and geometry in model physical systems (*3, 31, 32*) and blood cell suspensions (*33*). PGSE techniques using liquids can also provide microstructural information about a variety of heterogeneous systems, such as droplet size in emulsions and vesicles (*2*), and porosity in liquid-saturated reservoir rocks (*4, 15, 34–36*).

In this paper, we address three key issues on the path to employing laser polarized noble gas for time-dependent diffusion studies in porous media. First, we confirm the applicability of the Stejskal–Tanner PGSE technique and its variants to freely diffusing, thermally polarized gas samples. Second, we demonstrate for the first time the measurement of time-dependent diffusion of a thermally polarized gas in a porous medium. Finally, we investigate techniques that allow the measurement of time-dependent diffusion coefficients in laser polarized gas samples and discuss issues related to the measurement of restricted diffusion of laser polarized noble gas in porous media. Under Experimental Design and Pulse Sequences, we discuss the techniques used in all three sets of experiments, along with the need for non-standard methods when one is dealing with laser polarized gas samples. Under Results and Discussion, we present and analyze the results obtained from each of the three series of experiments listed above.

## EXPERIMENTAL DESIGN AND PULSE SEQUENCES

We performed noble gas NMR measurements using glass sample cells filled with known pressures of gas determined by a ratio method between the volume of a vacuum manifold and the sample cell. The samples cells had volumes of $\sim$80 cm$^3$ and were fitted with valves to allow variation of gas pressure or installation of model porous media (e.g., packed beads). Isotopically enriched xenon (90% $^{129}$Xe) was employed in all experiments using thermally polarized gas. For these thermally polarized experiments, we added oxygen gas ($O_2$) to all sample cells to reduce the $T_1$ of $^{129}$Xe from $\sim$1000 to $\sim$1 s and thus make signal averaging feasible. Our laser polarized noble gas experiments were performed with sealed glass cells of approximately 25 cm$^3$ in volume, and containing 3 atm pressure of natural abundance xenon gas ($\sim$27% $^{129}$Xe). Laser polarization was achieved by spin exchange collisions between the $^{129}$Xe atoms and optically pumped rubidium vapor. The sample cell was optically pumped at $\sim$90°C for approximately 30 min in the fringe field of a 4.7 T NMR magnet using $\sim$15 W of circularly polarized light at 795 nm from a fiber-optic-coupled diode laser array (manufactured by Optopower Corp, Tucson, AZ).

All NMR experiments were performed using a GE Omega/CSI spectrometer with a 4.7 T horizontal bore magnet. The spectrometer operated at 55.3 MHz for $^{129}$Xe, using a home-built solenoid RF coil, and its gradient coils provided up to 7 G/cm gradient strength. We implemented a standard Stejskal–Tanner PGSE pulse sequence (*23*) and a stimulated echo variant, PGSTE (*28*), illustrated in Fig. 1a, on the Omega system for diffusion coefficient determination in homogeneous gas systems. In heterogeneous media (e.g., beads or rocks), large background magnetic field gradients can be created in the sample due to the magnetic susceptibility mismatch between the gas and solid phases. These background gradients can greatly inhibit the precision and accuracy of standard pulsed-field-gradient diffusion measurements (*37*). However, variations of the PGSTE sequence have been developed (*37, 38*) to reduce this effect. Thus for measurements with thermally polarized xenon gas in heterogeneous media we adopted a modified Cotts 13-interval PGSTE sequence using bi-polar gradient pulses with a stimulated echo (*39*). A schematic of this sequence is given in Fig. 1 b. For the thermally polarized gas experiments, 8–16 signal averaging scans were used for free gas samples, while 32–64 were used for porous media samples.

The finite, non-renewable magnetization of laser polarized noble gas requires modification of standard NMR pulse sequences. Since the noble gas magnetization is induced by optical pumping, there is no "recovery" of magnetization within a $T_1$ time after an RF pulse. Instead, the noble gas magnetization is finite and lost once used. Hence, low flip angle experiments such as FLASH have been popular for imaging of laser polarized noble gas (*40*). However, as each pulse consumes magnetization, continued use of the same flip

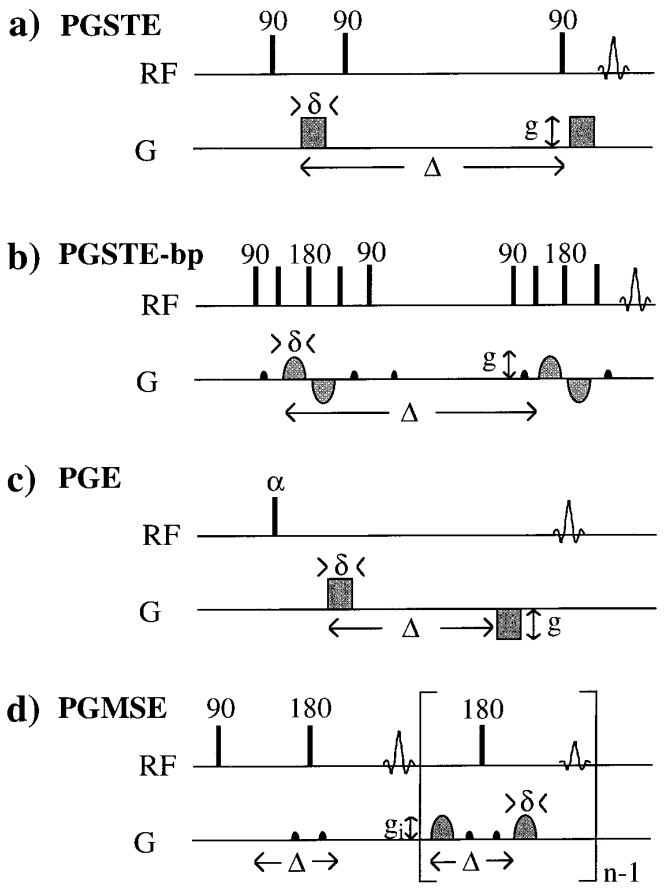


**FIG. 1.** Pulsed-field-gradient pulse sequences used for diffusion coefficient determinations in the work presented in this paper. In all four diagrams, $\delta$ is the gradient pulse time, $\Delta$ is the gas diffusion time, and $g$ is the strength of the applied gradient pulse. (a) A stimulated echo variant, referred to as PGSTE, of the standard Stejskal–Tanner Pulsed Gradient Spin Echo (PGSE) pulse sequence (*23*). (b) A modified PGSTE (stimulated echo) sequence incorporating bi-polar diffusion encoding gradient pulses (PGSTE-bp) to cancel out the effect of background gradients in heterogeneous media. 180° RF pulses are the three pulses between the first two pulses labeled as 90°; and the three pulses after the third pulse labeled as 90°. The small, dark-colored gradient pulses are clean-up and crusher gradients. (c) A low, variable flip-angle implementation of the Pulsed Gradient Echo (PGE) sequence. The RF flip angle $\alpha$ was increased for each shot, along with the value of $g$. (d) The Pulsed Gradient Multiple Spin Echo sequence, with the transverse magnetization refocused $n$ times to produce $n$ echoes in the train. The effect of the diffusion-encoding gradients $g_i$ are cumulative in this sequence. The small, dark-colored gradient pulses are clean-up gradients applied along an axis orthogonal to the diffusion-encoding direction.

angle RF pulse will deliver progressively less magnetization into the transverse plane. This effect can be compensated for by using a variable flip angle approach which progressively increases the flip angle throughout the experiment (*19, 40*). Unfortunately, low flip angle excitation techniques are very sensitive to slightly mis-set or spatially non-uniform 180° RF pulses. Thus PGSE experiments with low flip angle excitation are impractical with laser polarized noble gases because the spurious signal from non-uniform 180° RF pulses can exceed the signal from a low flip angle excitation pulse.

To overcome this problem, we have used two variations of the PGSE technique, described in the following, to measure the time-dependent diffusion of laser polarized noble gas.

*Pulsed Gradient Echo.* First, we employed a simple pulsed gradient echo (PGE) sequence (see Fig. 1c), that does not utilize 180° RF pulses—so problematic with low flip angle excitation. With this method, the sign of the second gradient pulse is reversed with respect to the first pulse to refocus the NMR signal in the absence of a 180° RF pulse. In other respects, however, the PGE and PGSE techniques are identical, including the ability to give time dependent diffusion information, as well as the data analysis procedure (*23*). We implemented the PGE technique using a variable flip-angle approach, where the flip-angle for the $n$th pulse, $\theta_n$, is given by (*19*)

$$(\sin^2\theta_{N-n})^{-1} = N - n + 1, \qquad [1]$$

and $N$ is the total number of RF pulses. Note that some of the techniques used recently (*19–21*) to measure diffusion of laser polarized noble gas are similar to the PGE technique, but with the key difference that these experiments had no delay between the gradient pulses; i.e., they are effectively constant gradient experiments (*22*) that do not provide information on time-dependent gas diffusion.

Gradient echo sequences are typically limited by fast, diffusion-induced decay of the transverse magnetization (i.e., $T_2^*$ decay), rather than by slower, homogeneous processes (i.e., $T_2$ decay) which limit spin-echo sequences. As a result, even in unrestricted, freely diffusing systems, the PGE technique can measure only moderate noble gas diffusion times ($\lesssim$100 ms), and thus can probe only moderate gas diffusion length scales ($\lesssim$500 $\mu$m for gas pressures of $\sim$1 atm). To circumvent this limitation, one needs to manipulate the transverse magnetization with fully refocusing RF pulses, as in the case of the spin or stimulated echo techniques. To do this refocusing effectively requires that all the large, laser polarized noble gas magnetization be in the transverse plane (to avoid spurious signal, radiation damping, etc.). However, the magnetization of a laser polarized noble gas sample is finite and not easily replenished, and a standard spin or stimulated echo sequence will consume all this magnetization. Thus standard methods can only provide information for a single diffusion encoding gradient value, whereas data for several such field gradients are needed to map out the echo attenuation curve and determine the gas diffusion coefficient for a particular diffusion time.

A single-shot diffusion technique that will provide a number of echoes with differing diffusion attenuation from a single RF excitation pulse is therefore required. A number of single-shot diffusion methods have been developed, most using combinations of spin and stimulated echoes resulting from a single RF

excitation pulse (*41–43*). Such a combination results, however, in the acquisition of echoes at differing diffusion times Δ, as well as differing gradient strengths. While such an approach is feasible for unrestricted diffusion where the diffusion coefficient will not vary with Δ, it is not suitable for the measurement of time-dependent diffusion. Instead, the method of Li and Sotak (*44, 45*), the Pulsed Gradient Multiple Spin Echo allows a series of echoes to be acquired at a constant Δ, but with varying diffusion encoding gradient values, and therefore should provide a method for time-dependent diffusion coefficient determination from laser polarized gases.

*Pulsed Gradient Multiple Spin Echo.* We have adapted the single-shot diffusion technique known as the Pulsed Gradient Multiple Spin Echo, or PGMSE (see Fig. 1d), for the determination of time-dependent diffusion coefficients of laser polarized noble gas. This technique allows the full echo attenuation curve to be determined from a single RF excitation, and is based on the continuous refocusing schemes used in CPMG echo trains (*22, 46*) and RARE Fast-Spin-Echo imaging (*47*). In the PGMSE sequence, transverse magnetization created by a single 90° RF excitation pulse is continually refocused by 180° RF pulses, providing a train of multiple echoes. A diffusion-encoding gradient pulse pair is applied during each echo cycle, with the result that each echo read out has a different diffusive attenuation. To guard against spurious signals from imperfect 180° pulses, small clean-up gradients in an axis orthogonal to the diffusion-encoding direction are applied around each 180° pulse.

The data acquisition and analysis procedure employed in a PGMSE experiment differs from the standard PGSE procedure (*23*). In a standard PGSE experiment, the data obtained with each successive diffusion-encoding gradient must be normalized against the data obtained in the absence of a diffusion-encoding gradient, in order to remove effects of $T_1$ or $T_2$ relaxation during the diffusion time Δ. Thus, it is usual to acquire a series of echoes, each with increasing diffusion gradient, with the first gradient value equal to zero. Then the analysis involves normalizing each echo height by the first (zero gradient) echo height. However, in the PGMSE technique, each refocused echo in the train is attenuated by $T_2$ *before* the diffusion encoding for that echo cycle occurs. In addition to $T_2$ effects, each echo in the PGMSE train is also attenuated by the diffusion-encoding gradients applied in previous echo cycles in the experiment. Thus, the diffusion-encoding gradient effect is cumulative, and the echo height for each echo $n$ is given by

$$S_n(g,t) = \exp\left(-\left(\sum_{i=1}^{i=n} g_i^2\right)\delta^2\gamma^2 D(\Delta\delta/3)\right)\exp(-t/T_2), \quad [2]$$

where $D$ is the free gas diffusion coefficient, $\delta$ is the gradient pulse width, Δ is the diffusion time, and $g_i$ is the strength of the applied diffusion gradient pulse during the $i$th echo in the PGMSE train.

In their original implementation of the PGMSE technique (*44, 45*), Li and Sotak derived the diffusion coefficient for water from a plot of the ratio of $n$th echo height to the $(n-1)$th echo, thus removing the $T_2$ contribution and the effect of previous gradients applied during the echo train. This assumes the gradient is being incremented evenly throughout the experiment. In our implementation with noble gas, we performed two PGMSE experiments, one without and one with the application of the diffusion-encoding gradients, and normalized the train of echoes from the second experiment to the first set of echoes. We analyzed our PGMSE data by creating a simple $\ln(S(t)/S(0))$ attenuation series for the two experiments with zero and finite diffusion gradients. A linear fit was made through the zero-gradient series, and the calculated $T_2$ attenuation was subtracted from the diffusion-attenuated data series. The resultant, normalized data were then analyzed in the standard Stejskal–Tanner manner (*23*), with the exception that each point in the attenuation series was plotted as a function of the sum of gradients applied in all echo cycles up to that point, rather than the gradient strength applied only for that echo. Due to the cumulative nature of the effect of the diffusion-encoding gradients, we found that better results were obtained by applying first zero, and then the same pulsed gradient value in each echo cycle, rather than increasing the gradient strength incrementally for each echo.

The weakness of the PGMSE technique is that, like the standard PGSE, refocusing with 180° RF pulses leaves the finite noble gas magnetization in the transverse plane throughout the experiment, and hence subject to $T_2$ decay, which in turn limits the maximum possible diffusion time Δ of an experiment (see discussion below of experimental results). To avoid such $T_2$ decay problems in a standard PGSE experiment, the 180° RF pulse is replaced by the two 90° pulses of a stimulated echo sequence. Unfortunately, the large number of secondary echoes produced by this technique, and the loss of magnetization as crusher gradients remove such echoes, makes this method extremely difficult to implement for multiple refocusing and the formation of an echo train. However, in parallel with this work, we have devised a single-shot diffusion technique that incorporates both a stimulated echo to remove the effects of $T_2$ decay and a variable Δ to enable time-dependent diffusion measurements. This technique is based on the BURST excitation method (*48*), and is best described by a different formalism; thus it is reported elsewhere (*49*).

## RESULTS AND DISCUSSION

We report three groups of gas diffusion experiments in this paper. First, we applied the standard PGSE technique and stimulated echo variants to thermally polarized xenon gas, and found that these techniques provide an efficient and accurate measure of the free gas diffusion coefficient. Second, we used

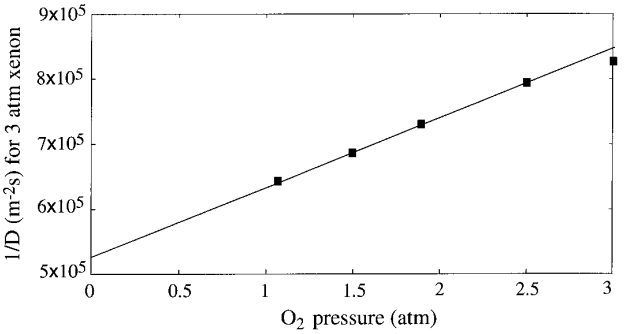


**FIG. 2.** Results of PGSE diffusion measurements for 3 atm thermally polarized xenon, as a function of $O_2$ partial pressure. A straight line fit for $1/D$ yields an extrapolated diffusion coefficient of $1.90 \times 10^{-6}$ m$^2$ s$^{-1}$ for 3 atm xenon and no $O_2$.

the bi-polar stimulated echo method to measure time dependent (i.e., restricted) diffusion of thermally polarized xenon gas in model porous systems (bead packs). The results of these restricted gas diffusion measurements were consistent with theoretical calculations (*35, 36*) and previous NMR experiments performed with water-saturated bead packs (*4*). Finally, we applied the two PGSE-derived techniques (the PGE and PGMSE sequences described above) to free thermally and laser polarized xenon gas, in the absence of glass beads, finding the PGMSE method to be superior to the PGE technique for efficiently measuring gas diffusion over a wide range of diffusion times. Note that all diffusion coefficient measurements reported in this paper have one standard deviation uncertainties (resulting from statistical error in straight line fits to echo attenuation data) that are less than 3%.

### *PGSE Techniques Applied to Unrestricted, Thermally Polarized Xenon Gas*

To demonstrate the robustness of the PGSE technique and variants when applied to gases, we made a series of measurements on a cell containing 3 atm thermally polarized xenon gas, isotopically enriched to 90% $^{129}$Xe, and 2 atm $O_2$. The xenon diffusion coefficients were measured in three ways: (i) with the standard PGSE sequence; (ii) with the standard stimulated echo PGSTE sequence; and (iii) using a modified PGSTE sequence incorporating bi-polar gradient pulses (*39*). All three methods covered a wide range of diffusion times ($\Delta$), ~75–1000 ms, with the gradient pulse time ($\delta$) kept constant and the maximum magnetic field gradient adjusted appropriately. The three methods gave the same value for the diffusion coefficient of 3 atm of xenon in 2 atm $O_2$ for all diffusion times: the average value from these three methods, over all values of $\Delta$, was $1.37 \times 10^{-6}$ m$^2$ s$^{-1}$.

To account for the presence of oxygen ($O_2$) in thermally polarized xenon samples, we measured the xenon diffusion coefficient as a function of $O_2$ partial pressure. These experiments were performed on gas samples consisting of 3 atm xenon gas, isotopically enriched to 90% $^{129}$Xe, and varying $O_2$ partial pressures ranging between 1 and 3 atm. Xenon diffusion coefficients were determined with the PGSE sequence; results are shown in Fig. 2. Plotting the inverse of the measured xenon diffusion coefficient ($D^{-1}$) versus $O_2$ partial pressure yields a straight line, with $D = 1.90 \times 10^{-6}$ m$^2$ s$^{-1}$ when the $O_2$ content is extrapolated to zero. Since gas diffusion coefficients scale inversely with gas pressure, the xenon self-diffusion coefficient at 1 atm pressure is determined from our data to be $5.71 \times 10^{-6}$ m$^2$ s$^{-1}$. This value agrees very well with previous theoretical calculations and measurements using a variety of non-NMR techniques (*50, 51*).

We also measured the xenon diffusion coefficient as a function of xenon partial pressure. These PGSE experiments were performed on gas samples consisting of 2 atm $O_2$ gas, and varying xenon partial pressures ranging between 1 and 3 atm. (Again, the xenon gas was isotopically enriched to 90% $^{129}$Xe.) Plotting the inverse of the measured xenon diffusion coefficient ($D^{-1}$) versus xenon partial pressure yields a straight line (see Fig. 3). The extrapolated value of the xenon diffusion coefficient at zero xenon pressure (infinite dilution) is the xenon-in-$O_2$ diffusion coefficient, which appears not to have been reported previously. At 2 atm $O_2$ pressure our measurements determine this diffusion coefficient to be $6.77 \times 10^{-6}$ m$^2$ s$^{-1}$. Note that this xenon-in-$O_2$ diffusion coefficient should also scale inversely with $O_2$ gas pressure.

### *Diffusion of Thermally Polarized Xenon Gas in Model Porous Systems*

In the second group of experiments, we determined the time-dependent (or restricted) diffusion coefficient of thermally polarized xenon gas imbibed in model porous media. We filled a glass cell completely with densely packed, randomly oriented 4 mm glass beads (obtained from Dow Chemical, New York), and then admitted 3 atm xenon gas, isotopically

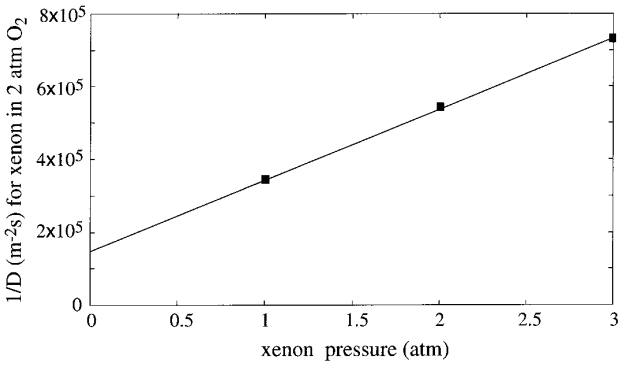


**FIG. 3.** Results of PGSE diffusion measurements for thermally polarized xenon in the presence of 2 atm $O_2$, as a function of xenon partial pressure. A straight line fit for $1/D$ yields an extrapolated diffusion coefficient of $6.77 \times 10^{-6}$ m$^2$ s$^{-1}$ for infinite dilution of xenon in 2 atm $O_2$.

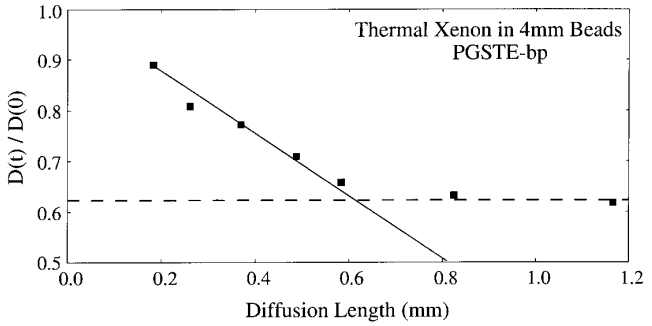


**FIG. 4.** Measured time-dependent diffusion coefficient ($D(t)$) for 3 atm thermally polarized xenon gas mixed with 2 atm $O_2$ and imbibed in a random pack of 4 mm glass beads. The values of $D(t)$ are normalized to the measured free diffusion coefficient, $D(0) = 1.37 \times 10^{-6}$ m$^2$ s$^{-1}$. The diffusion length $z$, plotted on the abscissa, is calculated from the diffusion time $\Delta$: $z = \sqrt{D(0) \times \Delta}$. The solid straight line shown in this figure is the theoretical short-time limit of Eq. [3], calculated using a surface to volume ratio $S/V_p = 9.79$ expected for dense random packed spheres (*35*). The dashed straight line is the theoretical long-time limit of Eq. [4], calculated using the porosity of dense packed beads of ~40% (*36*).

enriched to 90% $^{129}$Xe, and 2 atm $O_2$ gas, to fill the interstitial (pore) spaces between the beads. The time-dependent xenon diffusion coefficient, $D(t)$, was measured over a wide range of diffusion times ($\Delta$), ~12.5–1000 ms, using the modified PGSTE sequence incorporating bi-polar gradient pulses (*39*). (*Note.* $t$ and $\Delta$ here are interchangeable.) Typical results for $D(t)$ are shown in Fig. 4. At the shortest of diffusion times, the xenon diffusion coefficient was close to the measured value for the free gas mixture, $D(0) = 1.37 \times 10^{-6}$ m$^2$ s$^{-1}$, and then decreased along the theoretical straight line derived from the surface–volume ratio, $S/V_p$, in accordance with the theoretical equation for random bead packs (*35*),

$$D(t)/D(0) = 1 - \frac{4}{9\sqrt{\pi}} \frac{S}{V_p} \sqrt{D(0)t} + \vartheta(D(0)t). \qquad [3]$$

For long diffusion times, $D(t)$ approached a limiting value of approximately $0.64 \times D(0)$, which is consistent with calculations (*36*) and previous NMR measurements in water-saturated bead packs (*4*). This asymptotic, long-time value of $D(t)$ provides an indication of the porosity of the sample,

$$D(t)/D(0) \sim \sqrt{\phi}. \qquad [4]$$

(*Note.* $\phi \sim 0.36-0.40$ in random packs of spherical beads.) (*36*). These thermally polarized xenon measurements are part of an on-going study of time-dependent gas diffusion in porous media, the results of which will be reported in a future publication.

*Application of PGE and PGMSE Techniques to Unrestricted Diffusion of Both Thermally and Laser Polarized Xenon Gas*

In the third group of experiments we measured the free gas diffusion coefficient of both thermally and laser polarized xenon using the two modified pulsed-field-gradient techniques discussed above (PGE and PGMSE). While these techniques were devised for application with laser polarized gas, we felt it prudent to test their application first with thermally polarized samples, allowing direct comparison with standard PGSE techniques.

Using a 90° excitation pulse and a relaxation delay of approximately five $T_1$ times, we used the PGE technique to measure diffusion coefficients in a cell containing 3 atm thermally polarized xenon gas, isotopically enriched to 90% $^{129}$Xe, and 2 atm $O_2$. The xenon diffusion coefficient was measured at two different diffusion times, $\Delta = 50$ and 250 ms, with an average value of $1.40 \times 10^{-6}$ m$^2$ s$^{-1}$, in excellent agreement with the value of $1.41 \times 10^{-6}$ m$^2$ s$^{-1}$ obtained from our PGSE experiments conducted simultaneously with equivalent experimental parameters.

We then modified the PGE technique to incorporate variable-flip angle excitation, and used this technique to measure the diffusion coefficient of 3 atm of laser polarized xenon gas for two different diffusion times: $\Delta = 50$ and 100 ms. (Note that the longer diffusion time [100 ms] was shorter than that for the thermally polarized xenon PGE experiment [250 ms] because of the difficulty of shimming a laser polarized sample without consuming most of the sample's finite magnetization. Poor shimming of static field gradients results in a shorter $T_2^*$ and limits the maximum $\Delta$.) After standard Stejskal–Tanner analysis (see Fig. 5), the data yielded diffusion coefficients of $1.90 \times 10^{-6}$ and $1.91 \times 10^{-6}$ m$^2$ s$^{-1}$ for $\Delta = 50$ and 100 ms, respectively, showing good self-consistency as well as agreement with the diffusion coefficient that we obtained for 3 atm

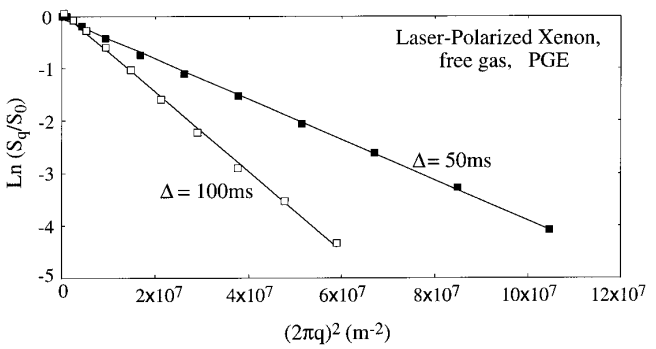


**FIG. 5.** Demonstration of the Pulsed Gradient Echo (PGE) technique for measurements of laser polarized xenon gas diffusion. A Stejskal–Tanner echo attenuation semi-log plot is shown for 3 atm laser polarized xenon gas at two different diffusion times, $\Delta = 50$ and 100 ms, yielding diffusion coefficients of $1.90 \times 10^{-6}$ and $1.91 \times 10^{-6}$ m$^2$ s$^{-1}$, respectively. Here $q$, plotted on the abscissa, is the wavenumber of the magnetization grating created by a particular diffusion-encoding gradient pulse ($g$): $q = (\gamma \delta g / 2\pi)$.

xenon gas by extrapolation of the thermally polarized data shown in Fig. 2 (extrapolated thermal data: $1.90 \times 10^{-6}$ m$^2$ s$^{-1}$). While giving excellent results, the limitations due to $T_2^*$ decay is obviously a drawback for the PGE technique. Attempts to use this technique for diffusion times longer than 100 ms yielded poor spectral data with resulting poor echo attenuation curves and inaccurate diffusion coefficients.

The PGMSE experiments were conducted on the same samples of thermally and laser polarized xenon gas as those used in the PGE tests just described. For both types of samples, the same applied gradients were used, namely zero gradient for the first echo in the train, followed by 3.17 G/cm gradient pulses for each of the remaining seven echoes acquired in the train. Diffusion times of $\Delta = 25$–$250$ ms were used for thermally polarized gas, and $\Delta = 25$–$500$ ms for the laser polarized gas. The gradient pulse length, $\delta$, was decreased from 3 to 0.6 ms as $\Delta$ was increased, keeping the total signal attenuation constant. The application of the PGMSE technique was identical for the thermal and laser polarized samples, with the exception that in the case of the thermally polarized sample, extensive signal averaging was carried out (~48 scans), while the laser polarized data were obtained with a single scan. Acquisition of the "zero gradient" PGMSE echo train followed immediately. For the thermal sample, this was done with similar signal averaging, but for the laser polarized sample, these data were acquired from the considerably lower residual signal remaining after the "finite gradient" experiment.

Sample echo attenuation curves from the PGMSE experiments for thermally and laser polarized xenon are shown in Fig. 6. The echo attenuation data for the longest time ($\Delta = 250$ ms for thermal gas, and $\Delta = 500$ ms for laser polarized gas) in each case is omitted for the sake of clarity. Averaged over five diffusion times, the diffusion coefficient for the thermally polarized xenon sample was found to be $1.35 \times 10^{-6}$ m$^2$ s$^{-1}$, in good agreement with standard PGSE experiments conducted simultaneously (which yielded an average value of $1.39 \times 10^{-6}$ m$^2$ s$^{-1}$). For the laser polarized xenon sample, the average over six diffusion times gave a diffusion coefficient of $1.89 \times 10^{-6}$ m$^2$ s$^{-1}$, also in excellent agreement with the extrapolation of PGSE thermal data shown in Fig. 2 and the PGE experiments described above. Note that for long diffusion times and large diffusion-encoding gradients (i.e., large echo attenuation), some of the thermally polarized PGMSE data deviated from a linear semi-log echo attenuation curve (see Fig. 6a) due to significant $T_2$ decay, in combination with diffusive attenuation, resulting in poor signal-to-noise. These echo attenuation data were excluded from fits for the xenon diffusion coefficient. Experiments also showed that when $\Delta$ was increased further such that $T_2$ was the dominant attenuation factor, the accuracy of the resultant diffusion coefficients was poor. Also, because of the combined signal attenuation due to both $T_2$ decay and diffusion encoding, 50% more signal averaging scans were acquired for the thermal PGMSE experiments than for the corresponding PGSE experiments. Nevertheless, the single-shot nature of the PGMSE technique resulted in nearly an order of magnitude reduction in overall experimental time, compared to the PGSE technique for thermally polarized xenon samples.

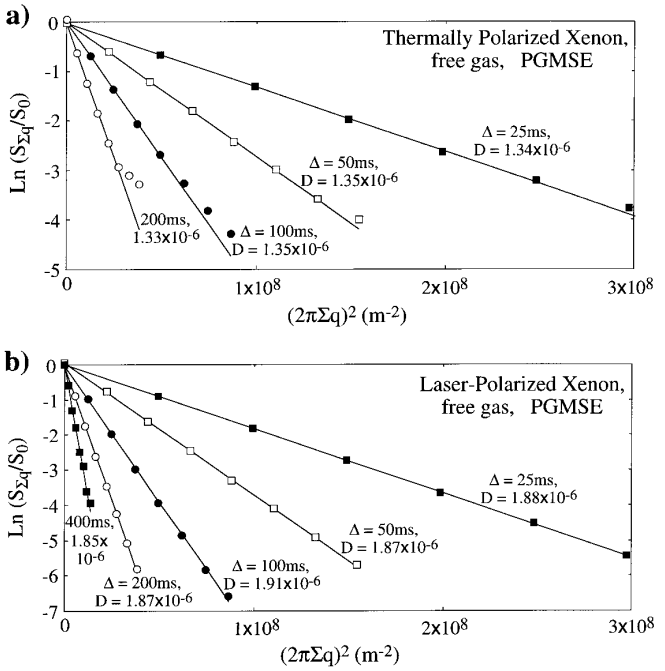


**FIG. 6.** Demonstration of the PGMSE technique for measurements of the diffusion of both thermally and laser polarized xenon gas. Stejskal–Tanner echo attenuation semi-log plots are shown for (a) 3 atm thermally polarized xenon gas mixed with 2 atm $O_2$ at four different diffusion times $\Delta = 25$–$200$ ms; and (b) 3 atm laser polarized xenon gas at five different diffusion times $\Delta = 25$–$400$ ms. For each diffusion time, the resultant diffusion coefficient is plotted next to the echo attenuation data. Here $\Sigma q$, plotted on the abscissa of both figures, is the effective wavenumber resulting from the cumulative effect of the multiple diffusion-encoding gradient pulses ($g_i$) employed in the PGMSE technique.

## CONCLUSION

The experiments reported in this paper demonstrate the utility of pulsed-field-gradient NMR methods for measurements of time dependent gas diffusion. Experiments were performed using thermally polarized xenon gas, in both an unrestricted and a restricted environment (packed beads), and with freely diffusing laser polarized xenon gas. First, we showed that standard pulsed-field-gradient techniques (PGSE and variants) provide efficient and accurate measures of free gas diffusion for thermally polarized xenon, with reproducible results over a wide range of diffusion times. Second, we showed that a modified stimulated echo sequence with bi-polar gradient pulses enables measurement of time-dependent diffusion of thermally polarized xenon gas imbibed in porous media. Third, we noted that the finite, non-renewable magnetization of laser polarized noble gas makes impractical the

execution of standard PGSE techniques for diffusion measurements of these special gases. While in principle such standard techniques could be implemented with low flip angle RF excitation, in practice, low flip angle methods are ineffective because of extreme sensitivity to slightly mis-set or spatially non-uniform 180° RF pulses. Thus we employed two modified PGSE techniques for measuring time-dependent diffusion of laser polarized noble gas: one that omits 180° RF pulses (the Pulsed Gradient Echo or PGE technique); and one that uses single-shot, multiple-spin echo data acquisition (the Pulsed Gradient Multiple Spin Echo or PGMSE technique). We tested these techniques with thermally and laser polarized xenon gas, and found the PGMSE technique to be superior to the PGE method, and to standard PGSE techniques and variants, for efficiently measuring free laser polarized noble gas diffusion over a wide range of diffusion times and, hence, lengths.

Finally, we note two important topics regarding time-dependent diffusion of laser polarized noble gas in heterogeneous systems (e.g., porous media) that are not addressed by the experimental work reported in this paper. First, the rationale for measuring the diffusion of noble gases rather than liquids through porous media is the ability of noble gases to diffuse rapidly through pores without loss of spin polarization (a result of the much larger gas diffusion coefficients and the much smaller surface depolarization probability of noble gas spins). However, rapid gas diffusion also creates the technical NMR problem of significant gas motion during the application of diffusion encoding gradient pulses. This technical problem is a breakdown of the "narrow pulse approximation," an assumption that is essential to the simplicity of the PGSE technique (and variants) used to measure time-dependent diffusion. It has recently been calculated (*52*) that when diffusion during an encoding pulse, $\sqrt{\delta D}$, exceeds $\sim 0.14a$, where $a$ is the average pore diameter in the porous medium, then the narrow pulse approximation breaks down, and systematic errors are introduced into the measurement of time-dependent (i.e., restricted) diffusion and the resultant characterization of the porous medium's microstructure. For example, for a 1 atm sample of laser polarized xenon gas ($D_{\text{free}} = 5.7 \times 10^{-6}$ m$^2$ s$^{-1}$) and a pulse width $\delta = 1$ ms, the narrow pulse approximation breaks down for pore diameters smaller than about 0.5 mm. Note that many porous media of interest (e.g., reservoir rocks and lung alveoli) have pore diameters that are smaller than 0.5 mm. Therefore, gas motion during diffusion-encoding pulses can be a significant limitation to the application of pulsed-field-gradient measurements of time-dependent noble gas diffusion as a probe of porous media microstructure. The recently devised multiple-propagator approach of Callaghan (*53*) may provide a method to account for gas diffusion during the encoding pulses. It may also be possible to circumvent this rapid gas diffusion problem with higher gas pressures (including buffer gases), or the use of low-inductance gradient coils to provide faster diffusion-encoding gradient pulses.

The second important topic still to be addressed is the large magnetic susceptibility mismatches in solid–gas heterogeneous systems, and the resultant effect on NMR measurements of time-dependent diffusion of imbibed, laser polarized noble gas. At typical NMR magnetic fields ($\sim$1 T) the spatially varying magnetic susceptibility of porous media creates large, local magnetic field gradients in the sample that can greatly shorten the $T_2$ and $T_2^*$ of the imbibed noble gas. For example, we measured the $T_2^*$ of laser polarized xenon gas imbibed in packed glass beads to be $\sim$5–10 ms, and the $T_2$ to be $\sim$20–30 ms (both measurements at 4.7 T). When $T_2$ becomes shorter than the diffusion time $\Delta$ (if the noble gas spins are left in the transverse plane during $\Delta$), or when $T_2^*$ becomes shorter than the diffusion-encoding gradient pulse train used in a multiply refocusing NMR diffusion measurement (like PGMSE), then pulsed-field-gradient techniques fail for laser polarized noble gas because of irretrievable loss of the sample's magnetization. Thus we found that for our 4.7 T system, the PGE and PGMSE techniques fail for laser polarized xenon imbibed in packed glass beads because the xenon $T_2$ is typically shorter than diffusion times that probe useful diffusion distances. In addition, our recently devised single-shot diffusion method, based on the BURST technique and described elsewhere (*49*), can also fail for laser polarized noble gas imbibed in heterogeneous systems due to the inability to refocus background gradients within this technique's constant gradient excitation scheme. In summary, NMR measurements of time-dependent diffusion of laser polarized noble gas in heterogeneous systems with large magnetic susceptibility gradients can be $T_2$- or $T_2^*$-limited in high-field NMR spectrometers. We expect that practical measurement of such time-dependent gas diffusion will require either: (i) lower magnetic fields, to reduce the background gradients and hence increase the noble gas $T_2$ and $T_2^*$; or (ii) gradient sets capable of stronger gradient output in pulse times considerably less than the $\sim$750 $\mu$s used in this study (to reduce the time required for the phase-encoding pulse train of a multiply refocusing experiment); or (iii) easily replenishable samples of laser polarized noble gas, to provide one sample per gradient value, with approximately six to eight such samples for the gradient values needed to determine the gas diffusion coefficient $D(\Delta)$ for a single diffusion time $\Delta$. We are currently investigating these possibilities.

## ACKNOWLEDGMENTS

We gratefully acknowledge scientific discussions with, and the technical assistance of, Martin Hurlimann, Lawrence Schwartz, Robert Kleinberg, and Glenn Wong. The work was supported by NASA Grant NAG5-4920, NSF Grant BES-9612237, Whitaker Foundation Grant RG 95-0228, and the Smithsonian Scholarly Studies Program.

## REFERENCES

1. P. Stilbs, *Prog. Nucl. Magn. Reson. Spectrosc.* **19,** 1 (1987).
2. O. Soderman and P. Stilbs, *Prog. Nucl. Magn. Reson. Spectrosc.* **26,** 445 (1994).

3. P. T. Callaghan, A. Coy, D. MacGowan, K. J. Packer, and F. O. Zelya, *Nature* **351,** 467 (1991).
4. L. L. Latour, P. P. Mitra, R. L. Kleinberg, and C. H. Sotak, *J. Magn. Reson. A* **101,** 342 (1993).
5. S. Mohanty and H. J. Bernstein, *J. Chem. Phys.* **53,** 461 (1970).
6. E. R. Hunt and H. Y. Carr, *Phys. Rev.* **130,** 2302 (1963).
7. P. A. Rinck, S. B. Petersen, and P. C. Lauterbur, *Fortschr. Rontgenstr.* **140,** 239 (1984).
8. M. J. Lizak, M. S. Conradi, and C. G. Fry, *J. Magn. Reson.* **95,** 548 (1991).
9. D. O. Kuethe, A. Caprihan, E. Fukushima, and R. A. Waggoner, *Magn. Reson. Med.* **39,** 85 (1998).
10. W. Happer, E. Miron, S. Schaefer, D. Schreiber, W. A. van Wijngaarden, and X. Zeng, *Phys. Rev. A* **29,** 3092 (1984).
11. M. S. Albert, G. D. Cates, B. Driehuys, W. Happer, B. Saam, C. S. Springer, Jr., and A. Wishnia, *Nature* **370,** 199 (1994).
12. J. R. MacFall, H. C. Charles, R. D. Black, H. L. Middleton, J. C. Swartz, B. Saam, B. Driehuys, C. Erickson, W. Happer, G. D. Cates, G. A. Johnson, and C. E. Ravin, *Radiology* **200,** 533 (1996).
13. G. Navon, Y-Q. Song, T. Room, S. Appelt, R. E. Taylor, and A. Pines, *Science* **271,** 1848 (1996).
14. P. T. Callaghan, "Principles of Nuclear Magnetic Resonance Microscopy," Oxford Univ. Press, Oxford (1991).
15. M. D. Hürlimann, K. G. Helmer, L. L. Latour, and C. H. Sotak, *J. Magn. Reson. A* **111,** 169 (1994).
16. G. R. Davies, T. K. Halstead, R. C. Greenhow, and K. J. Packer, *Chem. Phys. Lett.* **230,** 239 (1994).
17. S. Peled, F. A. Jolesz, C-H. Tseng, L. Nascimben, M. S. Albert, and R. L. Walsworth, *Magn. Reson. Med.* **36,** 340 (1996).
18. I. E. Dimitrov, S. R. Charagundla, R. Rizi, R. Reddy, and J. S. Leigh, Abstracts of the 5th ISMRM Annual Meeting, Vancouver, No. 1705 (1997).
19. B. R. Patyal, J-H. Gao, R. F. Williams, J. Roby, B. Saam, B. A. Rockwell, R. J. Thomas, D. J. Stolarski, and P. T. Fox, *J. Magn. Reson.* **126,** 58 (1997).
20. M. Bock, *Magn. Reson. Med.* **38,** 890 (1997).
21. D. M. Schmidt, J. S. George, S. I. Pentilla, A. Caprihan, and E. Fukushima, *J. Magn. Reson.* **129,** 184 (1997).
22. H. Y. Carr and E. M. Purcell, *Phys. Rev.* **94,** 630 (1954).
23. E. O. Stejskal and J. E. Tanner, *J. Chem. Phys.* **42,** 288 (1965).
24. M. Pfeffer and O. Lutz, *J. Magn. Reson. A* **113,** 108 (1995).
25. R. S. Ehrlich and H. Y. Carr, *Phys. Rev. Lett.* **25,** 341 (1970).
26. P. W. E. Peereboom, H. Luigjes, K. O. Prins, and N. J. Trappenhiers, *Physica B* **139–140,** 134 (1986).
27. P. W. E. Peereboom, H. Luigjes, and K. O. Prins, *Physica A* **156,** 260 (1989).
28. J. E. Tanner and E. O. Stejskal, *J. Chem. Phys.* **49,** 1768 (1968).
29. P. T. Callaghan, *Austr. J. Phys.* **37,** 359 (1984).
30. P. Stilbs, *Prog. Nucl. Magn. Reson. Spectrosc.* **19,** 1 (1987).
31. P. T. Callaghan, A. Coy, T. J. P. Halpin, D. MacGowan, K. J. Packer, and F. O. Zelya, *J. Chem. Phys.* **97,** 651 (1992).
32. A. Coy and P. T. Callaghan, *J. Chem. Phys.* **101,** 4599 (1994).
33. P. W. Kuchel, A. Coy, and P. Stilbs, *Magn. Reson. Med.* **37,** 637 (1997).
34. P. P. Mitra and P. N. Sen, *Phys. Rev. B* **45,** 143 (1992).
35. P. P. Mitra, P. N. Sen, and L. M. Schwartz, *Phys. Rev. B* **47,** 8565 (1993).
36. P. N. Sen, L. M. Schwartz, P. P. Mitra, and B. I. Halperin, *Phys. Rev. B* **49,** 215 (1994).
37. R. F. Karlicek and I. J. Lowe, *J. Magn. Reson.* **37,** 75 (1980).
38. R. M. Cotts, M. J. R. Hoch, T. Sun, and J. T. Markert, *J. Magn. Reson.* **83,** 252 (1989).
39. L. L. Latour, L. Li, and C. H. Sotak, *J. Magn. Reson. B* **101,** 72 (1993).
40. L. Zhao, R. Mulkern, C-H. Tseng, D. Williamson, S. Patz, R. Kraft, R. L. Walsworth, F. A. Jolesz, and M. S. Albert, *J. Magn. Reson. B* **113,** 179 (1996).
41. W. Sattin, T. H. Mareci, and K. N. Scott, *J. Magn. Reson.* **65,** 298 (1985).
42. F. Franconi, C. B. Snier, F. Seguin, L. Le Pape, and S. Akoka, *Magn. Reson. Imag.* **12,** 605 (1994).
43. F. Franconi, F. Lethimonnier, C. B. Snier, L. Pourcelot, and S. Akoka, *J. Magn. Reson. Imag.* **7,** 399 (1997).
44. L. Li and C. H. Sotak, *J. Magn. Reson.* **92,** 411 (1991).
45. L. Li and C. H. Sotak, *J. Magn. Reson. B* **101,** 8 (1993).
46. S. Meiboom and D. Gill, *Rev. Sci. Instrum.* **29,** 668 (1958).
47. J. Hennig, A. Nauerth, and H. Friedburg, *Magn. Reson. Med.* **3,** 823 (1986).
48. J. Hennig and M. Mueri, Abstracts of the 7th SMRM Annual Meeting, p. 238 (1988).
49. S. Peled, C-H. Tseng, A. A. Sodickson, R. W. Mair, R. L. Walsworth, and D. G. Cory, *J. Magn. Reson.* (1998), submitted for publication.
50. K. C. Hasson, G. D. Cates, K. Lerman, P. Bogorad, and W. Happer, *Phys. Rev. A* **41,** 3672 (1990).
51. J. O. Hirshfelder, C. F. Curtiss, and R. B. Bird, "Molecular Theory of Gases and Liquids," p. 581, Wiley, New York (1954).
52. L. Z. Wang, A. Caprihan, and E. Fukushima, *J. Magn. Reson.* **117,** 209 (1995).
53. P. T. Callaghan, *J. Magn. Reson.* **129,** 74 (1997).